Defect identification by load-dependence nonlinear ultrasonic phased array

Toshiki Yoshikawa[1‡], Kentaro Jinno[2], Taisei Ikemura[2], and Yoshikazu Ohara[1*]
([1]Tohoku Univ.; [2]Mitsubishi Heavy Industries)

1. Introduction

Thermal power generation currently plays an important role as a regulated power supply in Japan. Long-term operation of steam turbines (**Fig. 1**) can cause stress corrosion cracking (SCC) and corrosion pits. Specifically, the former can lead to catastrophic accidents such as blade failure. The identification of low-risk defects (i.e., corrosion pits) and high-risk defects (SCCs) would enable efficient operations. Specifically, this identification determines the viability of the remaining lifetime estimation of small and medium turbine rotors.

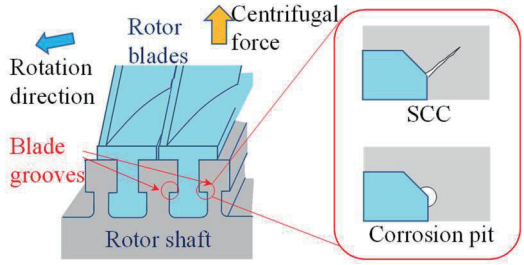

Fig. 1 Two types of defects generated in the steam turbines of thermal power plants.

In recent years, ultrasonic phased arrays (PA) have been applied for the nondestructive inspection of steam turbines. PA uses an array transducer with multiple piezoelectric elements, producing ultrasonic images via electrical scan. However, PA cannot identify the responses of an early-stage SCC (i.e., a depth of less than 1 mm) and a corrosion pit since those sizes are comparable. Note that the aforementioned PA is based on linear ultrasonics and can be referred to as linear ultrasonic PA.

As a different approach, nonlinear ultrasonic PA[1)] has been developed to image the closed cracks that are undetectable by linear ultrasonics. Given that nonlinear ultrasonics is based on the opening/closing vibrations of crack faces, it can also be applied to identify types of defects since such a phenomenon does not occur in non-crack defects such as corrosion pits.[2)] Among various nonlinear ultrasonic PAs utilizes large-amplitude incidence (MHz) to cause the crack opening/closing behaviors[1)], whereas the large amplitude is limited to be in the order of tens of nm. This might be insufficient for most cracked defects. To extend its applicability to various types of SCC, much higher displacement (stresses) would be required. To this end, the load difference phased array (LDPA)[3)] and global preheating and local cooling (GPLC)[4)] can be more effective since they can induce much higher displacement by their low-frequency loading. However, their applicability to SCC has yet to be investigated.

As a preliminary experiment for identifying SCC from corrosion pits, in this study, we investigate LDPA to specimens containing fatigue cracks and small round holes to prove the fundamental concept of defect identification.

E-mail: ‡toshiki.yoshikawa.t8@dc.tohoku.ac.jp,
*ohara@material.tohoku.ac.jp

2. Basic principles of selective visualization of cracks by load-dependence

A schematic illustration of LDPA for defect identification is shown in **Fig. 2**. Regardless of loading, a corrosion-pit response is constant in PA image (Figs. 2(a)-2(c)). Hence, the corrosion-pit response is canceled when the subtraction of the no-load PA image from that with loading, which is a core image processing of LDPA (Figs. 2(d) and 2(e)). In contrast, the SCC response in PA images can change depending on both tensile and compressive stresses since SCC may have both open and closed parts. That is, the tensile/compressive loading can make the crack open/closed from the original state, which results in an increase/decrease in the crack response (Figs. 2(f)-2(g)). Therefore, the LDPA can extract the crack as a positive and negative residue (Figs. 2(i) and 2(j)) for tensile and negative loading, respectively. The above principle allows selective visualization of SCC by LDPA.

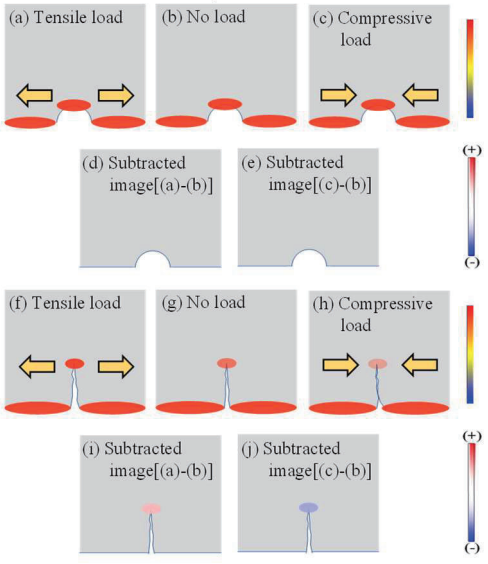

Fig. 2 Defect identification by LDPA.

3. Preliminary experiment of defect identification by LDPA

As a preliminary study, we applied LDPA with tensile loading to two aluminum-alloy (A7075) specimens (**Fig. 3**). One had the closed fatigue crack that was extended from a starting notch to a depth of 20 mm under the fatigue condition: a stress intensity factor range ΔK=15 MPa m$^{1/2}$ and a stress ratio R =0.067. The other one had a side-drilled hole (SDH) (ϕ1 mm) at a depth of 20 mm. Note that the SDH was not penetrated (3 mm from the side surface) to simulate a weak response of corrosion pits. The tensile load ranging from 0.1 to 8 kN was applied to each specimen. During the loading, PA images were obtained with a 1D array transducer (5 MHz, 32 elements). The imaging area is illustrated with a blue sector (angle: 20-60° (0.7° step), depth: 15-40 mm (3 mm step)).

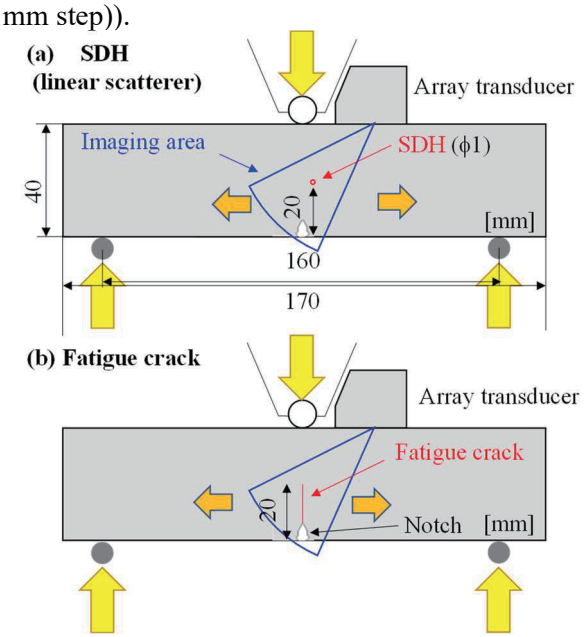

Fig. 3 Experimental configurations: (a) SDH and (b) fatigue-crack specimens.

Figure 4 shows the PA images obtained in the SDH and fatigue-crack specimens. For the SDH specimen, the SDH and the top of the notch were visualized in the PA image (Fig. 4(a)). However, no change was observed in the PA image regardless of loading (Figs. 4(a) and 4(b)). As a result of applying LDPA to those images, all the responses were successfully canceled (Fig. 4(c)). For the fatigue-crack specimen, weak fatigue-crack responses as well as a strong response at the top of the notch were visualized in the PA image (Fig. 4(d)). By applying the tensile load, the crack-tip response increased, whereas the notch response was constant (Figs. 4(d) and 4(e)). As a result of applying LDPA, the crack response was successfully extracted while the other scatterers were canceled (Fig. 4(f)). These results demonstrate the fundamental principle of LDPA for defect identification.

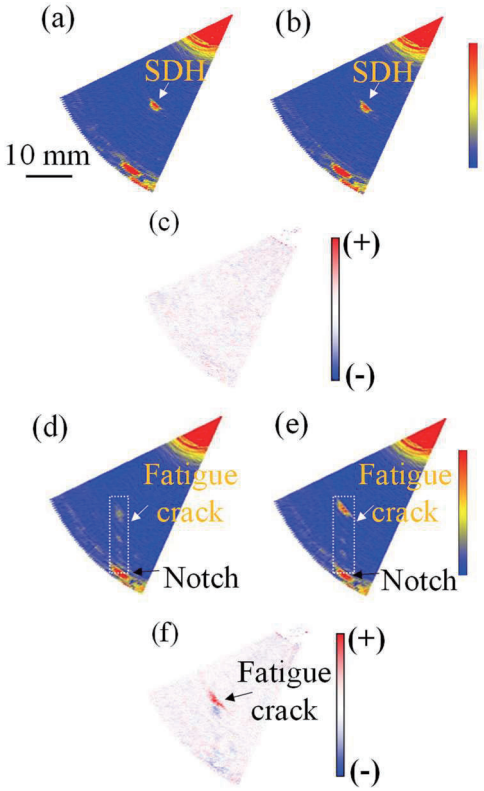

Fig. 4 PA and LDPA images: (a)-(b) PA images of SDH without and with tensile loading and (c) LDPA image (=(b)-(a)). (d)-(e) PA images of fatigue crack without and with tensile loading, and (f) LDPA image (=(e)-(d)).

5. Conclusions

As a preliminary experiment for the identification between SCC and corrosion pits, we demonstrated the basic performance of LDPA for defect identification. Although only the preliminary experiment was carried out using fatigue-crack and SDH specimens, we plan to apply LDPA with both tensile and compressive loading to realistic SCC specimens. In the future, mechanical loading will be replaced in a more practical way, thermal-stress loading (GPLC) for pragmatic application.

Acknowledgment

This work was supported by partially supported by JSPS KAKENHI (19K20910, 21H04592, and 22K18745) and JST FOREST Program (JPMJFR2023).

References

1) K.-Y. Jhang, C. J. Lissenden, I. Solodov, Y. Ohara, and V. Gusev, *Measurement of Nonlinear Ultrasonic Characteristics* (Springer, Singapore, 2020).
2) J. Potter, et al., PRL, **113** (2014) 144301.
3) Y. Ohara, et al., Ultrasonics, **51** (2011) 661.
4) Y. Ohara, et al., APL, **103** (2013) 031917.
5) Y. Ohara, et al., NDT&E Int., **91** (2017) 139.
6) Y. Ohara, et al., Ultrasonics, **119** (2022) 106629.